Evidence of Positronium Bloch States in Porous Crystals of Zn_{4}O-Coordination Polymers

Dhanadeep Dutta, Jeremy I. Feldblyum, David W. Gidley, James Imirzian, Ming Liu, Adam J. Matzger, Richard S. Vallery, and Antek G. Wong-Foy

Phys. Rev. Lett. **110**, 197403 — Published 10 May 2013

DOI: 10.1103/PhysRevLett.110.197403

Evidence of Positronium Bloch States in Porous Crystals of Zn_4O-Coordination Polymers

Dhanadeep Dutta[1,2], Jeremy I. Feldblyum[3,4], David W. Gidley[1,*], James Imirzian[1], Ming Liu[5,6], Adam J. Matzger[3,4], Richard S. Vallery[7], Antek G. Wong-Foy[3]

[1]Department of Physics, University of Michigan, 450 Church St., Ann Arbor, MI 48109, USA

[2]On leave of absence from Radiochemistry Division, Bhabha Atomic Research Centre, Trombay, Mumbai 400 085, India

[3]Department of Chemistry, University of Michigan, 930 N. University St., Ann Arbor, MI 48109, USA

[4]Macromolecular Science and Engineering, University of Michigan, 2300 Hayward Ave., Ann Arbor, MI, 48109-2136, USA

[5]NIST Polymers Division, 100 Bureau Dr. M/S 8541, Gaithersburg, MD 20899-8541, USA

[6]Nuclear Reactor Program, Department of Nuclear Engineering, North Caroline state University, P.O. Box 7909, Raleigh, NC, 27695, USA

[7]Department of Physics, Grand Valley State University, 151 Padnos Hall, Allendale, MI 49401, USA

PACS: 81.05.Rm, 36.10.Dr, 78.70.Bj

Abstract

Positronium (Ps) is shown to exist in a delocalized state in self-assembled metal-organic crystals that have large 1.3-1.5 nm cell sizes. Belonging to a class of materials with record high accessible specific surface areas, these highly porous crystals are the first to allow direct probing with simple annihilation lifetime techniques of the transport properties of long-lived triplet Ps in what is hypothesized to be a Bloch state. Delocalized Ps has unprecedented (high) Ps mobility driven primarily by weak phonon scattering with unusual and profound consequences on how Ps probes the lattice.

Positronium (Ps) is the hydrogen-like bound state of an electron with its antiparticle, the positron. Its ground state consists of spin singlet (p-Ps) and triplet states (o-Ps) that annihilate into two and three photons respectively with mean lifetimes of 0.125 ns and 142 ns [1]. Ps readily forms by electron capture when positrons are stopped in matter. In gases the Ps is free, interacting with the gas molecules only during collisions. In condensed matter Ps does not form in metals due to electron screening. In amorphous insulators Ps forms, localizes, and decays in open volume regions and is a well-known probe to characterize such "free" volume [2]. In some crystalline materials and within certain temperature limits p-Ps is observed in a delocalized Bloch state [3,4,5] but this is relatively rare and strong many-body effects can distort Ps and complicate interpretation. Such a novel quantum state of a single atom in a crystalline solid has also been observed for the heavier exotic atom of muonium [6], but only at very low temperatures (<10 mK). Recently a new class of crystalline materials called microporous coordination polymers, MCPs [7,8], has been synthesized that has nanometer-sized open volume networks that promote copious Ps formation [9]. We will show that triplet Ps in an MCP can be in a completely delocalized state consistent with a Bloch state throughout the temperature range from 77 K to 650K, thus enabling the exploration of Ps Bloch state decay and dynamics/transport using simple lifetime techniques.

MCPs are formed from the self-assembled linking together of metals or metal-oxide clusters and organic ligands ("linkers") of *controllable* nanometer lengths to form rigid, highly porous (open volumes up to 93% [10]) lattices with record-setting specific surface areas (>5000 m^2/g [10,11,12,13,14,15]). Development of MCPs over the last decade has attracted intense interest from both academic and industrial researchers [16] because of the transformative impact of this sorbent class for applications such as gas storage [14,15], separation [17] and catalysis [18]. O-Ps shows great promise as a unique, in-situ probe [9,19] of these new crystals. O-Ps lifetimes measured in MCPs are nominally consistent with the standard Tao-Eldrup model [20,21] and its extensions [22,23] in terms of deducing a mean free path in the porous network, but these models inherently treat Ps *localized* in at least two dimensions (eg., confined radially in a very long cylindrical pore). By ignoring the regularity of the highly open lattice the mobility of the Ps Bloch state and the startlingly long diffusion lengths that result and affect how Ps probes the material are lost. To realize its promising potential it is crucial to understand the quantum state in which Ps exists in MCPs.

We focus this letter on two MCPs called IRMOF-1 and IRMOF-8 (IRMOF refers to "isoreticular metal-organic framework," a MOF having the same net topology; see Fig. 1). The IRMOF series [24] consists of cubic-structured materials comprised of octahedral Zn_4O clusters linked together by linear dicarboxylates of variable length and chemical functionality. IRMOF-1 and IRMOF-8 are synthesized in our chemistry department and characterized for specific surface area, 3100 m^2/g and 4200 m^2/g, respectively, and crystallinity (sharp x-ray diffraction pattern). Both have individual grains that are transparent cubic single crystals with average side-length of 300 μm (see also supplementary information online). MCPs are analyzed by stopping positrons in them and measuring the lifetimes of o-Ps that annihilates both in and between the grains. The timing apparatus is similar to that reported in ref. [9]. We have two standard bulk PALS spectrometers and a variety of vacuum tight holders that permit vacuum and high pressure gas exposure, resistive heating, and LN_2 sample cooling. A ^{22}Na positron source of ~10 μCi is deposited on a tungsten foil and placed at the bottom of a well containing about 0.1 cm^3 of MCP crystals. The fraction of all positrons emitted from the source that annihilate as o-Ps is 35-40%.

The annihilation lifetime spectrum is generally well fitted with 3 lifetimes: a short lifetime less than 0.5 ns due to positron and p-Ps annihilation; a predominant o-Ps lifetime around 13.5 ns (IRMOF-1) or 18.5 ns (IRMOF-8) due to Ps annihilation within the crystal framework (72-90% of the o-Ps); and a long lifetime (roughly 80 ns in evacuated MOF) comprising 10–28% of all o-Ps decays. These framework lifetimes correspond in extended Tao-Eldrup annihilation models [22] to Ps mean free paths for annihilation of 1.3 nm and 1.5 nm, respectively; close to the mean free paths (1.5 nm and 1.8 nm) calculated from 4V/S where V and S are specific free volume and surface area from adsorption data [24]. Based on the same annihilation models Liu et al. [9] suggested that the 80 ns lifetime component in evacuated IRMOF-1 was due to Ps trapping in widely-spaced 6 nm diameter crystal defects. We will show that it is instead due to Ps diffusing out and escaping from the crystal grains and annihilating in the intergrannular open volume. This is both very surprising and revealing for two reasons: 1. It is surprising that Ps in such open interparticle volume with void size comparable to the 300 μm particle size, has such a *short* lifetime of 80 ns and not a value [22] much closer to that of Ps in free-space vacuum, 142 ns; and 2. Grain escape would require an extraordinarily long Ps diffusion length, ℓ, within the MCP grain of ~10 μm. This implies a diffusion constant, D, of order 100 cm^2/s; two orders of magnitude larger than Ps or positron diffusion constants reported for condensed matter

[25,26,27,28]. We will have to abandon the classical model of Ps diffusion in favor of a quantum mechanical treatment similar to that for treating electron conductivity and its temperature dependence in metals.

To show that the ~80 ns component is due to Ps escaping from the IRMOF-1 grains PALS spectra were acquired with the MCP exposed to helium and hydrogen gas pressures ranging from vacuum to 110 bar. Our focus is on the decay rate (1/lifetime) and relative intensity of the long-lived Ps component (the effect of gas exposure/adsorption on Ps annihilating in the framework will be presented elsewhere). Figure 2 shows this decay rate for He and H_2 gases at 296 K and 77 K as a function of gas density measured in Amagat (1 Amagat corresponds to the number density of Avogadro's number of molecules in the STP molar volume; ~1.08 Bar at 296 K). At densities > 0.1 Amagat the decay rate is consistent with that of Ps in pure gas (curves in Fig. 2). These decay rates extrapolate to nominally the vacuum o-Ps value, 0.007 ns^{-1} (1/142 ns). Were Ps annihilating in gas-filled, 6 nm lattice defects the gas dependent decay rates would extrapolate to 1/80 ns. The decay rates above 0.1 Amagat are completely consistent with Ps annihilating in the very large intergrannular volume while undergoing temperature (T) independent pick-off annihilation with the specific gas. So what is happening below 0.1 Amagat?

The unexpected rise in fitted Ps decay rate at the very lowest gas densities is expanded in the bottom graph of Fig 2. After scaling the H_2 density by a multiplicative factor of 2.5 *for both temperatures* the H_2 results then agree with the He results (to be discussed). Furthermore, if we scale the two 77 K curves by a factor of 3.3 (~T, not shown in figure) then all four curves would merge to a universal result! This unusual gas and temperature dependence can be explained by assuming that nominally thermalized Ps within the MCP grain diffuses to and escapes from the grain receiving an energy boost of E_0 so its total energy outside the grain is $E_0 + kT$ (E_0, on the scale of a zero point energy, might be 0.1 – 0.3 eV, [29,30]). Unhindered, such Ps would travel 20-30 mm making ~100 grain collisions and occasionally reenter a grain where annihilation occurs with higher rate corresponding to the 13 ns lifetime deep within the IRMOF-1 framework. The observed 80 ns Ps lifetime is then a time-weighted average of Ps subject to annihilation both inside (13 ns) and outside a grain (142 ns). The role of the gas is simply to degrade the Ps energy by an amount kT or more to below the E_0 *threshold* for grain reentry leaving Ps trapped in the

intergrannular space. We assume the energy lost per collision with a gas molecule of mass M_g is $\sim \frac{m}{M_g} E_0$ where m is the Ps mass, and hence the energy loss rate in a gas of density n_g is

$$\frac{dE}{dt} = \frac{m}{M_g} E_0 n_g \sigma_g v_0 \quad (1)$$

where σ_g is the collision cross section for Ps with the particular gas molecule and v_0 is the Ps velocity corresponding to E_0. To eliminate grain reentry after some time t (10 ns, the time we begin fitting the spectrum) we require the gas density to be high enough so that $\frac{dE}{dt} t \approx kT$ and therefore the required density, n_g^*, to decrease the fitted decay rate to that in the pure gas depends on temperature and gas as $n_g^* \sim \frac{M_g}{\sigma_g} T$. This linear dependence on T is evident in Fig. 2 (bottom), the 77 K results scaled by 3.3 (close to 296/77 = 3.8) merge with the 296 K results. The factor of 2.5 scaling in density of the H_2 data indicates

$$\frac{M_{He}}{\sigma_{He}} = 2.5 \frac{M_{H_2}}{\sigma_{H_2}}, \quad (2)$$

and, after accounting for the masses, we conclude $\sigma_{H_2} = 1.25\sigma_{He}$ at energy E_0. Based on direct cross section measurements [31] at energies > 5 eV this ratio is plausible. Indeed, given the difficulty in measuring Ps collision cross sections at sub-eV energies [32] it might be useful to use this new MCP-based method for accurately determining *relative* Ps momentum transfer cross sections for different gases.

The long-lived component in the PALS spectrum is thus the result of Ps escaping from the MCP grains and sometimes re-entering them if there is no buffer gas to slow down the Ps. As a lower limit on the fraction of Ps escaping from the grains, F_{esc}, we can simply use the fitted relative o-Ps intensity of this long-lived component which ranges in IRMOF-1 from ~16% at 296 K to 28% to 77 K (in vacuum). Assuming Ps is formed uniformly throughout a cubic particle of side length L the fractional volume within diffusion length $\boldsymbol{\ell}$ of a surface is $F_{esc} \sim 6\boldsymbol{\ell}/L$. F_{esc} of 16% and 28% correspond to $\boldsymbol{\ell}$ = 8-14 μm for particles with L = 300 μm. It is straightforward to

calculate the diffusion constant $D = {l^2}/{\tau}$ since τ =13.5 ns. Thus, D(77 K)~150 cm^2/s and D(296 K)~50 cm^2/s. Such large values for l and D in concert with longer diffusion at lower temperature are not consistent with classical diffusion. The argument for quantum diffusion in a Bloch state is compelling if we deduce the mean free path for Ps scattering with the lattice, £, and compare with the value of 1.5 nm determined from IRMOF-1 structure. Since $D = {v£}/{3}$ we can deduce £ if the average Ps diffusion velocity, v, is known. If we make the unsubstantiated assumption that Ps is thermalized then we deduce £(77 K)=1100 nm and £(296 K) =190 nm. Even if v is 10 times higher (unphysical Ps energy of 1-4 eV) £ is still 1-2 orders of magnitude larger than 1.5 nm.

To test this assertion of very long mean free paths for lattice scattering we again use He gas as an inert source of Ps scattering *within* the MCP framework to variably impede Ps diffusion and promote Ps thermalization. We consider F_{esc} vs. gas number density, n_{He}, at 77 K and 296 K. Actually, we have plotted in Figure 3 F_{esc} vs. $n_{He}\sigma_{He}$ where we have assumed a reasonable value (within a factor of 2) for σ_{He} =0.07 nm^2 [32] in order to provide an absolute length scale ($1/n_{He}\sigma_{He}$ is the mean free path for Ps between gas collisions). We can fit most of the data in Fig. 3 if we assume £ depends only on temperature, v is constant over the fitted gas density range, and gas collisions shorten the total Ps mean free path such that

$$F_{esc} \sim \frac{6l}{L} = \frac{6}{L}\sqrt{\frac{v\tau/3}{\frac{1}{£}+n_{He}\sigma_{He}}}. \qquad (3)$$

We exclude data below 0.001 nm^{-1} which correspond to the low density (< 0.1 Amagat) results shown in Fig. 2 that involve grain reentry (not a simple diffusion model). The fitted values of £ are 200 ±25 nm at 296 K and 425 ±50 nm at 77 K. The important point here is that £(T) is primarily determined by the gas scattering dependence (the shape of the curve) and not the absolute normalization term of $\sqrt{v\tau/3}$. We do find that this fitted velocity term is the same for 77 K and 296 K which suggests that Ps is only able to approach room temperature thermalization in the lattice. The agreement of this value of £(296 K) with the earlier value of 190 nm assuming thermal velocity supports this claim. Depending on our choice of σ_{He} these

values could change by a factor of two, but the inescapable fact is that the mean free path for scattering by lattice *imperfections* is 2 orders of magnitude larger than the 1.3 nm cell size of IRMOF-1. This unhindered propagation due to the coherent constructive interference of the scattered waves by a perfect lattice is a hallmark of Bloch states.

The temperature dependence of Ps escaping from the grains, F_{esc}, is shown for IRMOF-1 and IRMOF-8 in Fig. 4. The Ps lattice mean free path $\pounds$ should be the combined result of temperature dependent phonon scattering ($\pounds_{ph}$) and temperature independent defect scattering ($\pounds_{def}$);

$$\frac{1}{\pounds(T)} = \frac{1}{\pounds_{ph}(T)} + \frac{1}{\pounds_{def}}. \tag{4}$$

Assuming the phonon density n_{ph} will increase ~ linearly with T (the high temperature limit of the Bose-Einstein phonon distribution) the Ps-phonon scattering mean free path $\pounds_{ph} = 1/n_{ph}\sigma_{ph} \sim 1/T$. The curves shown in the figure are fits with this model that ignores any temperature dependence in the velocity term in F_{esc} (no Ps thermalization). This increase in the already long mean free path of Ps at low temperatures further illustrates the similarity with metallic electrical conductivity governed by phonon/defect scattering of Bloch electrons.

By way of temperature dependent gas exposure measurements in two MCPs we have shown that D~100 cm^2/s and the deduced mean free paths for Ps scattering with lattice phonons and defects are hundreds of nanometers. On the other hand, Ps annihilation determined by wave function overlap is perfectly consistent with the lattice scale lengths of ~1.5 nm. The simplest conclusion is that Ps is in a Bloch state manifested by a mean free path for scattering limited only by lattice imperfections. As a result the degree of crystalline imperfection of synthesized MCP will have wide ranging impact on the Ps annihilation lifetime spectrum both in terms of Ps diffusing and (not) thermalizing in the framework (fitted lifetime and intensity reduced by escape from the grain) and Ps moving amongst and reentering the grains (the lifetime and intensity of the long-lived Ps component). Study of this interesting delocalized atomic state is enabled by the recent availability of controllable nanometer lattice constant crystals and simplified by the minimal complexity of bulk lifetime techniques. In future work it would be interesting to perform angular correlation measurements on para-Ps annihilating in MCPs to determine if the

distinctive umklapp phonon peaks can be resolved [33]. Velocity spectroscopy [29] of the Ps emitted from the grains of varying IRMOF samples could check the lattice size dependence of the emission energy E_0. Relative Ps-gas collision cross sections for E_0 in the sub-eV range could help constrain divergent absolute measurements [32]. Further experiments on Ps Bloch state scattering from gases in the framework are also warranted to examine the applicability of plane wave cross sections determined in the pure gas. Finally, we need to improve our understanding of how this delocalized state of Ps is probing this important new class of MCP crystals.

The authors gratefully acknowledge technical help from William Frieze and helpful discussions with G. W. Ford and Roberto Merlin. This positron research was supported by the National Science Foundation (DMR-0907369) and the University of Michigan; and synthesis work was supported by the DOE (DE-SC0004888). JIF gratefully acknowledges support from the NSF Graduate Research Fellowship Program.

References:

∗ Author to whom correspondence should be addressed. E-mail: Gidley@umich.edu

[1] P. J. Schultz, and K. G. Lynn, Rev. Mod. Phys. **60**, 701 (1988).
[2] Y. C. Jean, Microchemical Journal **43**, 72 (1990).
[3] W. Brandt, G. Coussot, and R. Paulin, Phys. Rev. Lett. **23**, 522 (1969); A. Greenberger, A. P. Mills, A. Thompson, and S. Berko, Phys. Lett. 32A, 72 (1970).
[4] K. Inoue, N. Suzuki, I. V. Bondarev, and T. Hyodo, Phys. Rev. B **76**, 024304 (2007) and the references therein.
[5] B. Barbiellini, and P. M. Platzman, Phys. Status Solidi C **6**, 2523 (2009).
[6] R. Kadono, W. Higemoto, K. Nagamine, and F. L. Pratt, Phys. Rev. Lett. **83**, 987 (1999).
[7] B. F. Hoskins, and R. Robson, J. Am. Chem. Soc. **111**, 5962 (1989).
[8] G. Férey, Chem. Soc. Rev. **37**, 191 (2008).
[9] M. Liu, A. G. Wong-Foy, R. S. Vallery, W. E. Frieze, J. K. Schnobrich, D. W. Gidley, and A. J. Matzger, Adv. Mater. **22**, 1598 (2010).
[10] O. K. Farha, I. Eryazici, N. C. Jeong, B. G. Hauser, C. E. Wilmer, A. A. Sarjeant, R. Q. Snurr, S. T. Nguyen, A. O. Yazaydin, and J. T. Hupp, J. Am. Chem. Soc. DOI: 10.1021/ja3055639 (2012).
[11] K. Koh, A. G. Wong-Foy, and A. J. Matzger, J. Am. Chem. Soc. **131**, 4184 (2009).
[12] D. Yuan, D. Zhao, D. Sun, and H.-C. Zhou, Angew. Chem., Int. Ed. **49**, 5357 (2010).
[13] H. Furukawa, N. Ko, Y. B. Go, N. Aratani, S. B. Choi, E. Choi, A. Ö. Yazaydin, R. Q. Snurr, M. O'Keeffe, J. Kim, and O. M. Yaghi, Science **329**, 424 (2010).
[14] K. Sumida, D. L. Rogow, J. A. Mason, T. M. McDonald, E. D. Bloch, Z. R. Herm, T.-H. Bae, and J. R. Long, Chem. Rev. **112**, 724 (2012).

[15] T. K. Prasad and M. P. Suh, Chem. Eur. J. **18**, 8673 (2012).
[16] M. P. Suh, H. J. Park, T. K. Prasad, and D.-W. Lim, Chem. Rev. **112**, 782 (2012).
[17] J.-R. Li, J. Sculley, and H.-C. Zhou, Chem. Rev. **112**, 869 (2012).
[18] J. Y. Lee, O. K. Farha, J. Roberts, K. A. Scheidt, S. T. Nguyen, and J. T. Hupp, Chem. Soc. Rev. **38**, 1450 (2009).
[19] J. I. Feldblyum, M. Liu, D. W. Gidley, and A. J. Matzger, J. Am. Chem. Soc. **133**, 18257 (2011).
[20] S. J. Tao, J. Chem. Phys. **56**, 5499 (1972).
[21] M. Eldrup, D. Lightbody, J. N. Sherwood, Chem. Phys. **63**, 51 (1981)**.**
[22] T. L. Dull, W. E. Frieze, D. W. Gidley, J. N. Sun, and A. F. Yee, J. Phys. Chem. B **105**, 4657 (2001).
[23] B. Jasinska, A. L. Dawidowicz, T. Goworek, and J. Wawryszczuk, Opt. Appl. **33**, 7 (2003).
[24] M. Eddaoudi, J. Kim, N. Rosi, D. Vodak, J. Wachter, M. O'Keeffe, and O. M. Yaghi, Science **295**, 469 (2002).
[25] K. Ito, and Y. Kobayashi, Mat. Sci. Forum **445-446**, 307 (2004).
[26] M. Eldrup, A. Vehanen, P. J. Schultz, and K. G. Lynn, Phys. Rev. B **32**, 7048 (1985).
[27] S. Van Petegem, C. Dauwe, T. Van Hoecke, J. De Baerdemaeker, and D. Segers, Phys. Rev. B **70**, 113410 (2004).
[28] Y. C. Wu, J. Jiang, S. J. Wang, A. Kallis, and P. G. Coleman, Phys. Rev. B **84**, 064123 (2011).
[29] S. Mariazzi, P. Bettotti, and R. S. Brusa, Phys. Rev. Lett. **104**, 243401 (2010).
[30] D. B. Cassidy, P. Crivelli, T. H. Hisakado, L. Liszkay, V. E. Meligne, P. Perez, H. W. K. Tom, and A. P. Mills Jr., Phys. Rev. A **81**, 012715 (2010).
[31] S. J. Brawley, S. Armitage, J. Beale, D. E. Leslie, A. I. Williams, and G. Laricchia, Science **330**, 789 (2010).
[32] M. Skalsey, J. J. Engbrecht, C. M. Nakamura, R. S. Vallery, and D. W. Gidley, Phys. Rev. A **67**, 022504 (2003).
[33] Y. Nagai, M. Kakimoto, T. Hyodo, K. Fujiwara, H. Ikari, M. Eldrup, and A. T. Stewart, Phys. Rev. B **62**, 5531 (2000).

Figures and Captions

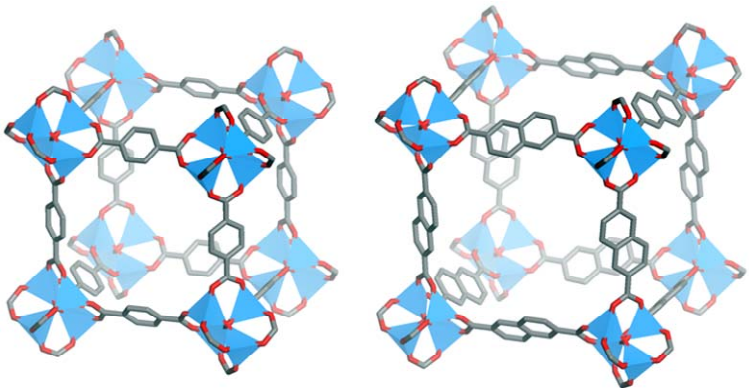

Fig. 1. (Color online) Models of IRMOF-1 (left) and IRMOF-8 (Zn, blue tetrahedra; O, red; C, gray. H atoms omitted for clarity). The cubic cell sizes are 1.292 nm and 1.505 nm, respectively.

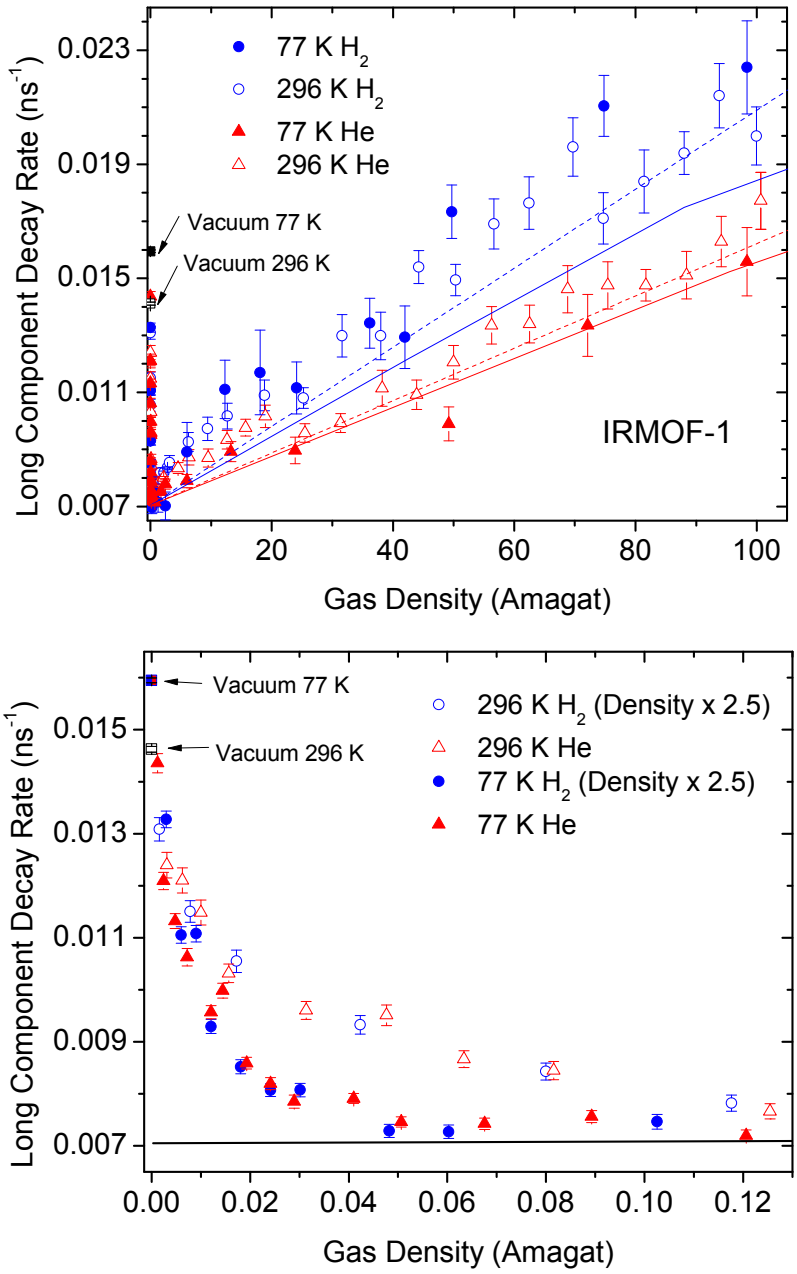

Fig. 2. (Color online) (Top) Long-lived component decay rate in IRMOF1 for He and H_2 gas at 77 K and 296 K. The solid/dashed curves are the o-Ps decay rates measured in the respective pure gases at 77 K and 296 K. The 77 K data continues the same trend to 400 Amagat. The unusual drop in the decay rate to that in the pure gases (solid line) at the lowest 0.1% of density are expanded in the lower graph. Both sets of H_2 data have been scaled by a multiplicative factor of 2.5 in density to account for its faster energy loss per collision than He.

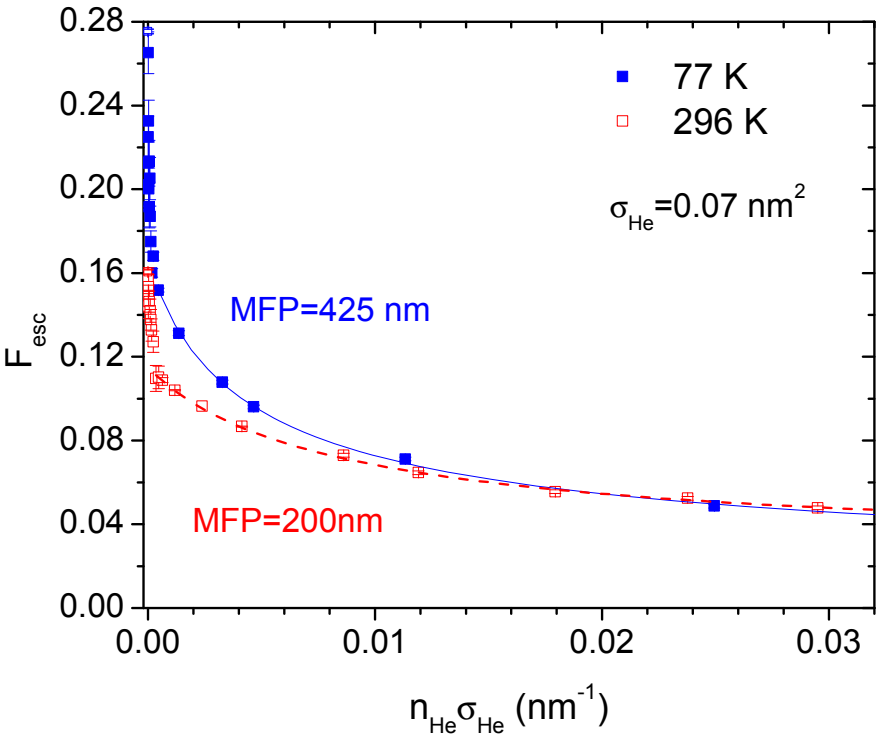

Fig. 3. (Color online) The fraction of Ps escaping the IRMOF-1 grain vs. gas density (multiplied by a nominal value for the Ps-He cross section, σ_{He} = 0.07 nm^2). The smooth curves are fits to a simple diffusion model that incorporates the variable gas scattering mean free path, $1/n_{He}\sigma_{He}$, with a temperature dependent mean free path for scattering with the lattice. Points on the far left are excluded from fitting as discussed in text.

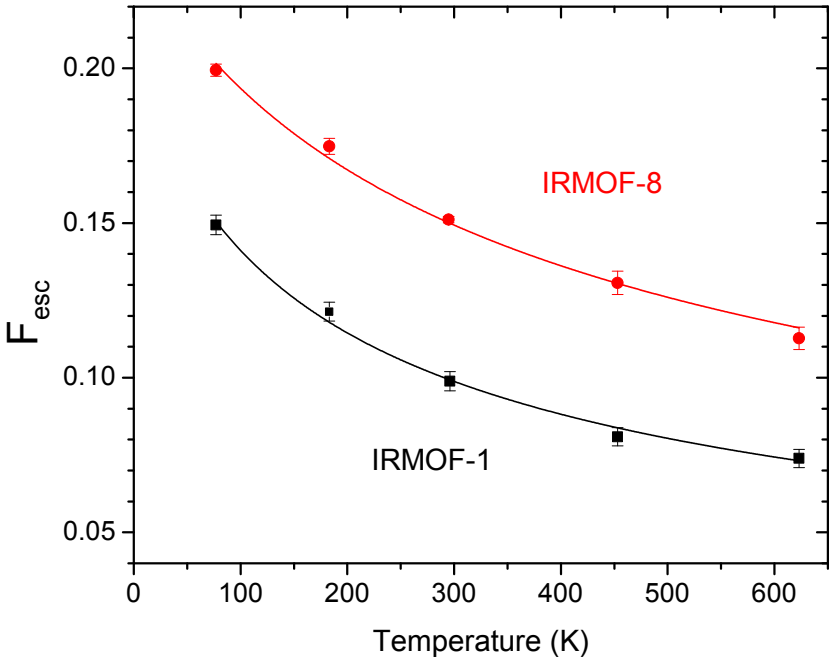

Fig. 4. (Color online) The temperature dependence of Ps escaping evacuated IRMOF-1 and IRMOF-8 grains. For IRMOF-8 F_{esc} has been divided by a factor of 2.3 = 300μm/130μm to account for its enhanced escape from smaller 130 μm grains. The smooth curves are fits to a diffusion model with a Ps-phonon mean free path that varies as $1/T$ and with a Ps-defect mean free path that is constant.